In-plane and out-of-plane bending vibration analysis of the laminated composite beams using higher-order theories

Ramazan-Ali Jafari-Talookolaei[1*]

[1]Babol Noshirvani University of Technology, Babol, Iran
[*]Corresponding author: ramazanali@gmail.com

ARTICLE INFO

DOI:10.46223/HCMCOUJS.acs.en.14.2.55.2024

Received: May 28th, 2024

Revised: June 13th, 2024

Accepted: July 10th, 2024

Keywords:

free vibration; higher-order theories; in-plane; laminated composite beam; out-of-plane

ABSTRACT

In this paper, relatively new higher-order shear deformation theories are presented for a thorough analysis of the in-plane and out-of-plane vibrational characteristics of laminated composite beams. Through the introduction of new displacement fields and the consideration of rotary inertia and Poisson's effect, the kinetic and potential energies of the beams have been derived. This formulation, displaying significant generality, accommodates arbitrary stacking sequences. Utilizing the finite element method, a new element has been presented for calculating the beam's vibrational characteristics. Featuring three nodes, each with seven degrees of freedom, this higher-order element provides a detailed representation of complex behaviors. Mass and stiffness matrices were derived using the energy method, and boundary conditions were applied through the penalty approach. The results exhibit a good degree of consistency and alignment with those obtained from the 3D commercial software ANSYS, validating the accuracy and reliability of the proposed methodology for structural analysis. This comprehensive approach contributes to advancing the understanding and modeling of laminated composite beams in diverse engineering applications. The effects of different parameters on the in-plane and out-of-plane vibration analysis of laminated composite beams have been investigated in detail.

1. Introduction

Vibration analysis of laminated composite beams plays a vital role in various engineering applications, offering valuable insights into the structural integrity, performance, and safety of complex structures. Laminated composite beams are extensively employed in aerospace, automotive, civil and mechanical engineering, and marine industries due to their superior strength-to-weight ratio and tailored physical properties. Vibration analysis of laminated composite beams is crucial for identifying natural frequencies, mode shapes, and potential resonance issues, allowing engineers to optimize designs and prevent structural failures. Additionally, it serves as an early warning system for damage detection and structural health monitoring, ensuring the safety and reliability of critical components in industries like aerospace.

In the vibration analysis of laminated composite beams and due to their composite nature, they often exhibit complex deformation patterns involving both in-plane and out-of-plane movements, so it is crucial to account for out-of-plane deformation alongside the in-plane deformation. Additionally, higher-order displacement fields provide a more accurate

representation of the beam's deformation behavior. Considering both out-of-plane deformation and higher-order displacement fields in the analysis ensures a more comprehensive and precise understanding of the beam's vibrational characteristics, leading to improved engineering designs and structural performance.

Numerous studies have explored the in-plane free vibration analysis of laminated composite beams (Alazwari, Mohamed, & Eltaher, 2022; Aydogdu, 2006; Bui, Nguyen, Nguyen, & Vo, 2022; Chandrashekhara, Krishnamurthy, & Roy, 1990; Chandiramani, Librescu, & Shete, 2002; Jafari-Talookolaei, Abedi, Kargarnovin, & Ahmadian, 2012; Hijmissen & Van Horssen, 2008; Kant & Gupta, 1988; Kant, Marur, & Rao, 1998; Karama, Afaq, & Mistou, 2003; Kim, Kim, Ri, Paek, & Kim, 2021; Krishnaswamy, Chandrashekhara, & Wu, 1992; Matsunaga, 2001, 2002; Nguyen, Nguyen, Vo, & Thai, 2020; Pavan, Muppidi, & Dixit, 2022; Ren, Cheng, Meng, Yu, & Zhao, 2021; So, Yun, Ri, Ryongsik, & Yun, 2021; Subramanian, 2006; Zhen & Wanji, 2008), whereas relatively few have delved into the in-plane and out-of-plane free vibration analyses (Boukhalfa, Hadjoui, & Cherif, 2008; Jafari-Talookolaei, Abedi, & Attar, 2017; Jafari-Talookolaei et al., 2022; Seraj & Ganesan, 2018). In the following paragraphs, the various deformation theories employed in these research works, including classical, first-order, and higher-order shear deformation theories, will be reviewed.

A higher-order shear-deformable beam model theory has been formulated by Kant and Gupta (1988). This theory encompasses both linear and quadratic variations of transverse normal strain and transverse shearing strain along the thickness of the beam. The impacts of transverse normal and shear stresses are integrated into the material's constitutive law. The finite element method has been employed to derive the solution. Chandrashekhara et al. (1990) conducted a study on the free vibration of a symmetrical laminated composite beam. Their analysis incorporated first-order shear deformation theory and rotary inertia, while Poisson's effect has been omitted. The study provides solutions for the free vibration of symmetrically laminated composite beams. Dynamic equations governing the free vibration of laminated composite beams have been derived through the application of Hamilton's principle by Krishnaswamy et al. (1992). In their formulation, the effects of transverse shear, rotary inertia, and Poisson's effect have been taken into account. Analytical solutions have been obtained using the method of Lagrange multipliers, wherein the free vibration problem has been treated as a constrained variational problem, with constraints introduced through Lagrange multipliers. To showcase the effectiveness of this methodology, natural frequencies and mode shapes of both clamped-clamped and clamped-supported composite beams are presented. Importantly, the results highlight the significant role played by the Poisson's effect in achieving accurate outcomes.

Kant et al. (1998) introduced an analytical solution for the natural frequency analysis of laminated composite beams using a higher-order refined theory. This theory integrates cubic axial, transverse shear, and quadratic transverse normal strain components into its fundamental formulation. Moreover, it characterizes each lamina layer as orthotropic and in a two-dimensional plane stress state. The analysis of the natural frequencies and buckling stresses in laminated composite beams has been done by considering the full influence of transverse shear and normal stresses, as well as rotatory inertia effects (Matsunaga, 2001). Using a power series expansion method for displacement components, a set of fundamental dynamic equations based on a one-dimensional higher-order theory for laminated composite beams under axial stress has been obtained.

Chandiramani et al. (2002) conducted the analysis of the in-plane free vibrations in rotating composite beams by employing a higher-order shear formulation. This study included

the presentation of linearized dynamical equations and numerical findings related to the problem of free vibration. To provide a comprehensive assessment, the results obtained using the present higher-order shearable model have been compared with those derived from existing first-order shearable and non-shearable structural models. Stresses and displacements in laminated composite beams under lateral pressures have been analyzed using a comprehensive global higher-order beam theory by Matsunaga (2002). This advanced theory effectively incorporates the influence of both transverse shear and normal stresses. To derive the foundational equilibrium equations for a one-dimensional higher-order theory applicable to laminated composite beams, the method of power series expansion of displacement components is employed, grounded in the principle of virtual work. Subsequently, a series of truncated approximate theories are employed to address boundary value problems for simply supported laminated composite beams.

Karama et al. (2003) studied the various higher-order beam theories and subjected them to comparative analysis. This assessment has encompassed investigations into their free vibration properties, as well as comprehensive examinations of bending and buckling behaviors. Vibration analysis of angle-ply laminated beams under various boundary conditions has been conducted by Aydogdu (2006). This investigation has relied on the application of a three-degrees-of-freedom shear deformable beam theory. The natural frequencies of free vibrations have been determined using the Ritz method, with the three displacement components being represented as straightforward algebraic polynomial series.

Subramanian (2006) studied the free vibration analysis of laminated composite beams, utilizing two higher-order displacement-based shear deformation theories and corresponding finite elements. Both theories have adopted quintic and quartic variations for in-plane and transverse displacements within the beams' thickness coordinates. The key distinction between the two theories lies in their treatment of transverse shear stress distribution. The first theory assumes a non-parabolic variation, while the second theory adopts a parabolic distribution. The equations of motion have been derived via Hamilton's principle, and two-node C_1 finite elements with eight degrees of freedom per node based on these theories for the free vibration analysis of the beams have been introduced. Zhen and Wanji (2008) evaluated multiple displacement-based theories by examining both the free vibration and buckling characteristics of laminated beams with arbitrary configurations, as well as soft-core sandwich beams. Analytical solutions for all the scenarios under consideration have been derived using Navier's method, involving the solution of eigenvalue equations.

The transverse vibrations of a stationary, uniform Timoshenko beam were investigated by Hijmissen and Horssen (2008). This beam experienced a linearly varying compression force due to gravity and its own weight. It is important to note that this compression force, while relatively small, cannot be considered negligible. To tackle this problem, approximations for the solution using a perturbation method based on multiple time scales were developed. Jafari-Talookolaei et al. (2012) investigated the free vibration analysis for a generally laminated composite beam, employing the Timoshenko beam theory. This analysis comprehensively considered the impact of material couplings, including bending-tension, bending-twist, and tension-twist couplings, while also accounting for the effects of shear deformation, rotary inertia, and Poisson's effect. This analysis has been carried out through the application of the method of Lagrange multipliers, wherein the free vibration problem is formulated as a constrained variational problem. As a result, analytical expressions for the natural frequencies and mode shapes of the system have been presented.

Utilizing the foundational equations of elasticity theory, a novel unified beam model was formulated for laminated composite beams by Nguyen et al. (2020). This model adopts a unified displacement field, which has been designed to seamlessly transition into existing shear deformation beam theories found in the literature. The governing equations are solved to determine deflections, stresses, natural frequencies, and critical buckling loads of composite beams. This analysis encompasses various boundary conditions and lay-ups and incorporates innovative hybrid trigonometric functions. Kim et al. (2021) presented a semi-analytical method for analyzing the forced vibration of cracked laminated composite beams. The model is based on the Timoshenko beam theory and solved dynamically using the Jacobi-Ritz method. To address boundary conditions at both ends of the composite laminated beam, the artificial elastic springs have been employed. For analyzing the dynamic characteristics of the CLCB, all allowable displacement functions are expressed in a generalized form, employing classical Jacobi orthogonal polynomials. The accuracy of the approach through a comparison with results has been obtained from the finite element method (utilizing ABAQUS software).

A novel third-order zigzag model tailored for both asymmetric and symmetric laminated composite beams was introduced by Ren et al. (2021). Within the context of a general displacement framework, a fresh zigzag shear strain shape function has been proposed. This function incorporated layerwise coefficients encompassing constant, linear, quadratic, and cubic terms. The free vibration characteristics of arbitrarily shaped laminated composite beams under generalized elastic boundary conditions were investigated by So et al. (2021). The Haar wavelet discretization method has been employed to analyze these vibrations. The Timoshenko beam theory serves as the fundamental model for the free vibration behavior of the Laminated Composite Beam (LCB). The present approach involves dividing the LCB into multiple segments, after which the displacement for each segment through the Haar wavelet series and subsequent integration has been determined.

Pavan et al. (2022) presented a computational approach for analyzing laminated beams by employing classical laminated theory, first-order shear deformation theory, and higher-order shear deformation theory. Each of these kinematic theories has been utilized to develop computational methods for analyzing laminated composite beams, applying the Isogeometric Analysis with Collocation (IGA-C) method. A mathematical model was developed by Alazwari et al. (2022) to predict the dynamic response of a laminated composite beam under varying axial loads, utilizing a third higher-order shear deformation beam theory. The geometrical kinematic relations of displacements have been described using the higher parabolic shear deformation beam theory. The distribution of the variable axial load has been accomplished along the axial direction through constant, linear, and parabolic functions. The variable coefficients-differential equations of motion have been discretized in the spatial direction using the numerical differential quadrature method. A comprehensive higher-order shear deformation theory tailored for the buckling and free vibration analysis of thin-walled composite I-beams was presented by Bui et al. (2022). This theory builds upon a unified nonlinear variation of shear strains across the wall thickness. To address various boundary conditions, series-type solutions employing hybrid shape functions, enhancing the versatility of the present approach for practical applications, have been developed.

Boukhalfa et al. (2008) studied the dynamic performance of a rotating composite shaft mounted on rigid bearings. Both in-plane and out-of-plane deformations of the composite shaft have been taken into account. To analyze the natural frequencies of the rotating composite shaft, a hierarchical beam finite element with six degrees of freedom per node has been developed in this

investigation. Dynamic instability analysis on doubly-tapered cantilever composite beams subjected to periodic rotational velocity was investigated by Seraj and Ganesan (2018). The analysis encompasses three types of vibrations: out-of-plane bending (flap), in-plane bending (lag), and axial vibrations. To investigate these vibrations, the Rayleigh-Ritz method and classical lamination theory, in conjunction with an energy-based formulation, have been employed.

Novel formulations for analyzing the in-plane and out-of-plane vibrations in both non-rotating and rotating laminated composite beams were introduced by Jafari-Talookolaei et al. (2017), Jafari-Talookolaei et al. (2022), respectively. These formulations take into account material couplings, Poisson's effect, shear deformation, and rotary inertia. The study presents both analytical and finite element solutions for these comprehensive analyses.

As the literature review indicates, the in-plane vibrations of laminated composite beams have been extensively studied. However, both in-plane and out-of-plane vibrations of composite beams have received much less attention, with most studies primarily using first-order shear deformation theory. Therefore, this paper introduces relatively new higher-order shear deformation theories for analyzing the in-plane and out-of-plane free vibrations of laminated composite beams. The subsequent sections cover several key aspects of this research. Firstly, the new displacement fields and their corresponding formulations are presented. Following that, a finite element solution for addressing the problem is introduced. Finally, the numerical results are compared with outcomes obtained from the commercial software ANSYS to validate the accuracy and efficiency of our modeling approach.

2. Mathematical modelling

Figure 1 illustrates a laminated composite beam characterized by its length (L), thickness (h), and width (b). The right-handed coordinate system (xyz) is situated at the left end of the beam.

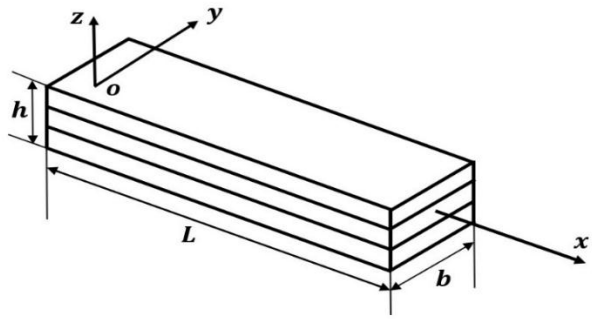

Figure 1. Schematic Representation of the laminated composite beam

The following higher-order displacement field has been considered:

$$u(x,y,,z,t) = u_0(x,t) - zw_{0,x} - yv_{0,x} + f(z)\,\psi(x,t) + g(y)\,\theta(x,t)$$
$$v(x,y,,z,t) = v_0(x,t) \tag{1}$$
$$w(x,y,,z,t) = w_0(x,t)$$

In which $u, v,$ and w are the displacement of an arbitrary point in the x-, y-, and z-directions, respectively. Furthermore, $u_0, v_0,$ and w_0 are the corresponding values of the beam's midplane, ψ and θ are variables to capture the magnitude of the cross-sectional distortion (Groh & Weaver, 2015), t is the time and:

Type 1: $f(z) = \frac{z}{2}\left[\frac{h^2}{4} - \frac{z^2}{3}\right]$ $g(y) = \frac{y}{2}\left[\frac{b^2}{4} - \frac{y^2}{3}\right]$ (2-a)

Type 2: $f(z) = z\left[1 - \frac{4z^2}{3h^2}\right]$ $g(y) = y\left[1 - \frac{4y^2}{3b^2}\right]$ (2-b)

Type 3: $f(z) = \frac{h}{\pi}\sin(\frac{\pi z}{h})$ $g(y) = \frac{b}{\pi}\sin(\frac{\pi y}{b})$ (2-c)

Type 4: $f(z) = h\sinh\left(\frac{z}{h}\right) - z\cosh\left(\frac{1}{2}\right)$ $g(y) = b\sinh\left(\frac{y}{b}\right) - y\cosh\left(\frac{1}{2}\right)$ (2-d)

Type 5: $f(z) = z\,e^{-2(z/h)^2}$ $g(y) = y\,e^{-2(y/b)^2}$ (2-e)

In Equation 1 and the subsequent equations, the comma represents differentiation with respect to the variable that follows it.

It should be noted that the higher-order functions described above have previously been employed by other researchers for in-plane analysis (Ambartsumyan, 1958; Belabed, Tounsi, Bousahla, et al., 2024; Bui, Tounsi, Do, Nguyen, & Phung, 2024; Dao et al., 2023; Karama et al., 2003; Meftah et al., 2024; Mesbah et al., 2023; Pham, Nguyen, & Tounsi, 2022; Reddy, 1986; Soldatos, 1992; Touratier, 1991), but in this context, they are applied for out-of-plane analysis.

It should be noted that there are other higher-order theories that have been examined by others (Belabed, Tounsi, Al-Osta, Tounsi, & Minh, 2024; Lakhdar et al., 2024) in the analysis of in-plane vibrations of beams, but they have been disregarded in this article.

Using the strain-displacement relations, the non-zero strains are as follows:

$$\begin{aligned}\gamma_x = u_{,x} &= u_{0,x} - zw_{0,xx} - yv_{0,xx} + f(z)\psi_{,x} + g(y)\,\theta_{,x} \\ &= \gamma_x^0 + z\kappa_{1x} + y\kappa_{2x} + f(z)\kappa_{3x} + g(y)\,\kappa_{4x}\end{aligned} \quad (3\text{-a})$$

$$\gamma_{xy} = u_{,y} + v_{,x} = g_{,y}\theta \quad (3\text{-b})$$

$$\gamma_{xz} = u_{,z} + w_{,x} = f_{,z}\psi \quad (3\text{-c})$$

in which:

$$\gamma_x^0 = u_{0,x}, \quad \kappa_{1x} = -w_{0,xx}, \quad \kappa_{2x} = -v_{0,xx}, \quad \kappa_{3x} = \psi_{,x}, \quad \kappa_{4x} = \theta_{,x} \quad (4)$$

Considering the Poisson's effect, the modified stress-strain relations can be obtained as (Jafari-Talookolaei et al., 2017):

$$\begin{Bmatrix}\sigma_x \\ \tau_{xy}\end{Bmatrix}^{(k)} = \begin{bmatrix}\bar{\bar{Q}}_{11} & \bar{\bar{Q}}_{16} \\ \bar{\bar{Q}}_{16} & \bar{\bar{Q}}_{66}\end{bmatrix}^{(k)} \begin{Bmatrix}\varepsilon_x \\ \gamma_{xy}\end{Bmatrix}^{(k)} \quad (5\text{-a})$$

$$\tau_{xz}{}^{(k)} = \bar{\bar{Q}}_{55}{}^{(k)}\gamma_{xz}{}^{(k)} \quad (5\text{-b})$$

Where:

$$\bar{\bar{Q}}_{11} = \bar{Q}_{11} - \frac{\bar{Q}_{12}{}^2}{\bar{Q}_{22}}, \qquad \bar{\bar{Q}}_{16} = \bar{Q}_{16} - \frac{\bar{Q}_{12}\bar{Q}_{26}}{\bar{Q}_{22}}, \qquad \bar{\bar{Q}}_{66} = \bar{Q}_{66} - \frac{\bar{Q}_{26}{}^2}{\bar{Q}_{22}} \tag{6-a}$$

$$\bar{\bar{Q}}_{55} = \bar{Q}_{55} - \frac{\bar{Q}_{45}{}^2}{\bar{Q}_{44}} \tag{6-b}$$

In which $\bar{Q}_{ij}$ is the reduced stiffness of the k^{th} layer (Reddy, 2004).

Strain potential energy can be written as:

$$U = \frac{1}{2}\int_0^L \int_{-b/2}^{b/2} \int_{-h/2}^{h/2} \left(\sigma_x{}^{(k)}\varepsilon_x{}^{(k)} + \tau_{xy}{}^{(k)}\gamma_{xy}{}^{(k)} + \tau_{xz}{}^{(k)}\gamma_{xz}{}^{(k)}\right) dz\, dy\, dx \tag{7}$$

Substituting equation 3 into equation 7, we have:

$$\begin{aligned} U = \frac{1}{2}\int_0^L \int_{-b/2}^{b/2} \int_{-h/2}^{h/2} \Big(&\sigma_x{}^{(k)}(\varepsilon_x^0 + z\kappa_{1x} + y\kappa_{2x} + f(z)\kappa_{3x} + g(y)\,\kappa_{4x}) \\ &+ \tau_{xy}{}^{(k)}\left(g_{,y}\theta\right) + \tau_{xz}{}^{(k)}\left(f_{,z}\psi\right)\Big)\, dz\, dy\, dx \end{aligned} \tag{8}$$

We can define the below resultant forces and moments:

$$\begin{Bmatrix} N_x \\ N_{xy} \\ M_{1x} \\ M_{2x} \\ M_{3x} \\ M_{4x} \\ Q_{xz} \end{Bmatrix} = \int_{-b/2}^{b/2} \int_{-h/2}^{h/2} \begin{Bmatrix} \sigma_x{}^{(k)} \\ \tau_{xy}{}^{(k)} g_{,y} \\ \sigma_x{}^{(k)} z \\ \sigma_x{}^{(k)} y \\ \sigma_x{}^{(k)} f(z) \\ \sigma_x{}^{(k)} g(y) \\ \tau_{xz}{}^{(k)} f_{,z} \end{Bmatrix} dz\, dy \tag{9}$$

Upon substituting equations 3 and 5 into equation 9 and performing some calculations, we obtain the below expressions for resultant forces and moments:

$$\begin{Bmatrix} N_x \\ N_{xy} \\ M_{1x} \\ M_{2x} \\ M_{3x} \\ M_{4x} \\ Q_{xz} \end{Bmatrix} = \begin{bmatrix} A_{11} & A_{16}^{g,y} & B_{11} & 0 & A_{11}^{f} & A_{11}^{g} & 0 \\ A_{16}^{g,y} & A_{66}^{g,y^2} & B_{16}^{g,y} & A_{16}^{yg,y} & A_{16}^{fg,y} & A_{16}^{gg,y} & 0 \\ B_{11} & B_{16}^{g,y} & D_{11} & 0 & B_{11}^{f} & B_{11}^{g} & 0 \\ 0 & A_{16}^{yg,y} & 0 & (b^2/12)A_{11} & 0 & A_{11}^{yg} & 0 \\ A_{11}^{f} & A_{16}^{fg,y} & B_{11}^{f} & 0 & A_{16}^{f^2} & A_{16}^{fg} & 0 \\ A_{11}^{g} & A_{16}^{gg,y} & B_{11}^{g} & A_{11}^{yg} & A_{16}^{fg} & A_{16}^{g^2} & 0 \\ 0 & 0 & 0 & 0 & 0 & 0 & A_{55}^{f,z^2} \end{bmatrix} \begin{Bmatrix} \varepsilon_x^0 \\ \theta \\ \kappa_{1x} \\ \kappa_{2x} \\ \kappa_{3x} \\ \kappa_{4x} \\ \psi \end{Bmatrix} \tag{10}$$

Where:

$$\begin{aligned}&\left(A_{ij}^{F}, B_{ij}^{F}\right)=\int_{-\frac{h}{2}}^{\frac{h}{2}}\int_{-\frac{b}{2}}^{\frac{b}{2}}\bar{\bar{Q}}_{ij}^{(k)}F(1,z)\,dy\,dz \qquad (i,j=1,6),(i=j=5)\\&D_{11}=\frac{b}{3}\sum_{k=1}^{n_t}\bar{\bar{Q}}_{11}^{(k)}({z_{k+1}}^{3}-{z_k}^{3})\end{aligned} \tag{11}$$

Where z_k and z_{k+1} represent the distances from the bottom and top faces of the k^{th} layer, respectively, in relation to the midplane.

Equation 8 can be written as:

$$U=\frac{1}{2}\int_0^L\left[N_x\varepsilon_x^0+M_{1x}\kappa_{1x}+M_{2x}\kappa_{2x}+M_{3x}\kappa_{3x}+M_{4x}\kappa_{4x}+N_{xy}\theta+Q_{xz}\psi\right]dx \tag{12}$$

By employing the equations 10 and 4 into equation 12, we have:

$$\begin{aligned}U=\tfrac{1}{2}\int_0^L\Big[&A_{11}u_{0,x}^2+A_{66}^{g,y^2}\theta^2+D_{11}w_{0,xx}^2+\tfrac{b^2}{12}A_{11}v_{0,xx}^2+A_{11}^{f^2}\psi_{,x}^2+A_{11}^{g^2}\theta_{,x}^2+\\&2A_{16}^{g,y}u_{0,x}\theta-2B_{11}u_{0,x}w_{0,xx}+2A_{11}^{f}u_{0,x}\psi_{,x}+2A_{11}^{g}u_{0,x}\theta_{,x}-2B_{16}^{g,y}w_{0,xx}\theta-\\&2A_{16}^{yg,y}\theta v_{0,xx}+2A_{16}^{fg,y}\theta\psi_{,x}+2A_{16}^{gg,y}\theta\theta_{,x}-2B_{11}^{f}\psi_{,x}w_{0,xx}-2B_{11}^{g}\theta_{,x}w_{0,xx}-\\&2A_{11}^{yg}\theta_{,x}v_{0,xx}+2A_{11}^{fg}\theta_{,x}\psi_{,x}+A_{55}^{f_z^2}\psi^2\Big]dx\end{aligned} \tag{13}$$

The kinetic energy can be written as:

$$T=\frac{1}{2}\int_0^L\int_{-b/2}^{b/2}\int_{-h/2}^{h/2}\rho^{(k)}\left(u_{,t}^2+v_{,t}^2+w_{,t}^2\right)dz\,dy\,dx \tag{14}$$

By substituting the displacement field, equation 1, into equation 14, we have:

$$\begin{aligned}T=\tfrac{1}{2}\int_0^L\Big[&I_1\left(u_{0,t}^2+v_{0,t}^2+w_{0,t}^2\right)+I_3w_{0,xt}^2+I_1\tfrac{b^2}{12}v_{0,xt}^2+I_1^{f^2}\psi_{,t}^2+I_1^{g^2}\theta_{,t}^2-\\&2I_2u_{0,t}w_{0,xt}+2I_1^{f}u_{0,t}\psi_{,t}+2I_1^{g}u_{0,t}\theta_{,t}-2I_2^{f}w_{0,xt}\psi_{,t}-2I_2^{g}w_{0,xt}\theta_{,t}-\\&2I_1^{yg}v_{0,xt}\theta_{,t}+2I_1^{fg}\theta_{,t}\psi_{,t}\Big]dx\end{aligned} \tag{15}$$

In which:

$$\left(I_1^F, I_2^F\right)=\int_{-\frac{h}{2}}^{\frac{h}{2}}\int_{-\frac{b}{2}}^{\frac{b}{2}}\rho^{(k)}F(1,z)\,dy\,dz,\quad I_3=\frac{b}{3}\sum_{k=1}^{n_t}\rho^{(k)}({z_{k+1}}^{3}-{z_k}^{3}) \tag{16}$$

3. Finite element solution

To obtain the numerical solution for the current problem, we employ a higher-order beam element as depicted in Figure 2. This one-dimensional element features three nodes located at $x = 0, L_e/2$, and L_e, and it comprises 21 Degrees Of Freedom (DOFs), specifically, 7 DOFs per node. These include axial displacement u_0, lateral and vertical deflections v_0, w_0, their spatial derivatives $v_{0,x}$, $w_{0,x}$, and two independent rotations, ψ and θ. The displacement fields for this higher-order beam element can be expressed as follows:

$$u_0 = [N_u]\{\delta\} = [N_1(\xi) \;\; 0 \;\; 0 \;\; 0 \;\; 0 \;\; 0 \;\; 0 \;\; N_2(\xi) \;\; 0 \;\; 0 \;\; 0 \;\; 0 \;\; 0 \;\; 0 \;\; N_3(\xi) \;\; 0 \;\; 0 \;\; 0 \;\; 0 \;\; 0 \;\; 0]\{\delta\} \tag{17-a}$$

$$v_0 = [N_v]\{\delta\} = [0 \;\; H_1(\xi) \;\; \bar{H}_1(\xi) \;\; 0 \;\; 0 \;\; 0 \;\; 0 \;\; 0 \;\; H_2(\xi) \;\; \bar{H}_2(\xi) \;\; 0 \;\; 0 \;\; 0 \;\; 0 \;\; 0 \;\; H_3(\xi) \;\; \bar{H}_3(\xi) \;\; 0 \;\; 0 \;\; 0 \;\; ($$ (17-b)

$$w_0 = [N_w]\{\delta\} = [0 \;\; 0 \;\; 0 \;\; H_1(\xi) \;\; \bar{H}_1(\xi) \;\; 0 \;\; 0 \;\; 0 \;\; 0 \;\; 0 \;\; H_2(\xi) \;\; \bar{H}_2(\xi) \;\; 0 \;\; 0 \;\; 0 \;\; 0 \;\; 0 \;\; H_3(\xi) \;\; \bar{H}_3(\xi) \;\; 0 \;\; ($$ (17-c)

$$\psi = [N_\psi]\{\delta\} = [0 \;\; 0 \;\; 0 \;\; 0 \;\; 0 \;\; N_1(\xi) \;\; 0 \;\; 0 \;\; 0 \;\; 0 \;\; 0 \;\; 0 \;\; N_2(\xi) \;\; 0 \;\; 0 \;\; 0 \;\; 0 \;\; 0 \;\; 0 \;\; N_3(\xi) \;\; 0]\{\delta\} \tag{17-d}$$

$$\theta = [N_\theta]\{\delta\} = [0 \;\; 0 \;\; 0 \;\; 0 \;\; 0 \;\; 0 \;\; N_1(\xi) \;\; 0 \;\; 0 \;\; 0 \;\; 0 \;\; 0 \;\; 0 \;\; N_2(\xi) \;\; 0 \;\; 0 \;\; 0 \;\; 0 \;\; 0 \;\; 0 \;\; N_3(\xi)]\{\delta\} \tag{17-e}$$

Here, ξ represents the intrinsic coordinate, defined as $\xi = \frac{x}{L_e}$. The Lagrange interpolation functions $N_i(x)$ and the Hermite interpolation functions $H_i(x)$ and $\bar{H}_i(x)$, where *i* ranges from 1 to 3, are provided as follows:

$$N_1 = 2(\xi - 0.5)(\xi - 1), \qquad N_2 = 4\xi(1 - \xi), \qquad N_3 = 2\xi(\xi - 0.5) \tag{18-a}$$

$$H_1 = (1 + 6\xi)\big(2(\xi - 0.5)(\xi - 1)\big)^2, \qquad \bar{H}_1 = 4\xi L_e(\xi - 0.5)^2(\xi - 1)^2 \tag{18-b}$$

$$H_3 = \big(1 - 6(\xi - 1)\big)\big(2\xi(\xi - 0.5)\big)^2, \qquad \bar{H}_3 = L_e(\xi - 1)(2\xi(\xi - 0.5))^2$$

$$H_2 = (-4\xi(\xi - 1))^2, \qquad \bar{H}_2 = L_e(\xi - 0.5)(4\xi(\xi - 1))^2 \tag{18-c}$$

(18-d)

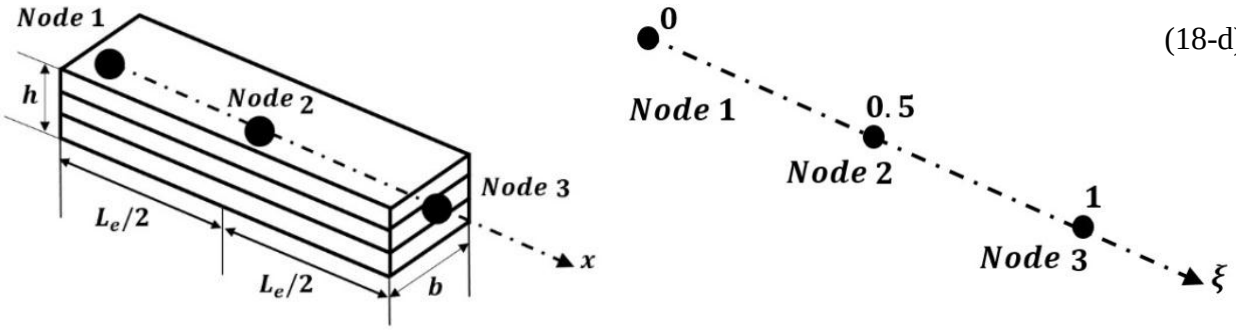

(a) (b)

Figure 2. (a) Higher order beam element and (b) its intrinsic coordinates

The vector representing the degrees of freedom for the beam element is denoted as:

$$\{\delta\} = \{u_{01}, v_{01}, v_{01,x}, w_{01}, w_{01,x}, \psi_1, \theta_1, u_{02}, v_{02}, v_{02,x}, w_{02}, w_{02,x}, \psi_2, \theta_2, u_{03}, v_{03}, v_{03,x}, w_{03}, w_{03,x}, \psi_3, \theta_3\}^T \quad (19)$$

In the equations above and those following, the superscript T signifies the transpose of a vector or matrix. Following a similar procedure as described in Jafari-Talookolaei et al. (2017) and substituting equation 17 into equation 13, and then integrating over the element length, the potential energy of a typical element can be formulated in terms of the displacement vector as:

$$U_e = \frac{1}{2}\{\delta\}^T[K_e]\{\delta\} \quad (20)$$

Here, $[K_e]$ represents the element stiffness matrix, which can be defined as:

$$\begin{aligned}[K_e] = \int_0^1 \Bigg[& \frac{A_{11}}{L_e^2}[N_{u,\xi}]^T[N_{u,\xi}] + A_{66}^{g,y^2}[N_\theta]^T[N_\theta] + \frac{D_{11}}{L_e^4}[N_{w,\xi\xi}]^T[N_{w,\xi\xi}] \\ & + \frac{b^2}{12}\frac{A_{11}}{L_e^4}[N_{v,\xi\xi}]^T[N_{v,\xi\xi}] + \frac{A_{11}^{f^2}}{L_e^2}[N_{\psi,\xi}]^T[N_{\psi,\xi}] + \frac{A_{11}^{g^2}}{L_e^2}[N_{\theta,\xi}]^T[N_{\theta,\xi}] \\ & + \frac{A_{16}^{g,y}}{L_e}\left([N_{u,\xi}]^T[N_\theta] + [N_\theta]^T[N_{u,\xi}]\right) - \frac{B_{11}}{L_e^3}\left([N_{u,\xi}]^T[N_{w,\xi\xi}] + [N_{w,\xi\xi}]^T[N_{u,\xi}]\right) \\ & + \frac{A_{11}^{f}}{L_e^2}\left([N_{u,\xi}]^T[N_{\psi,\xi}] + [N_{\psi,\xi}]^T[N_{u,\xi}]\right) + \frac{A_{11}^{g}}{L_e^2}\left([N_{u,\xi}]^T[N_{\theta,\xi}] + [N_{\theta,\xi}]^T[N_{u,\xi}]\right) \\ & - \frac{B_{16}^{g,y}}{L_e^2}\left([N_\theta]^T[N_{w,\xi\xi}] + [N_{w,\xi\xi}]^T[N_\theta]\right) - \frac{A_{16}^{yg,y}}{L_e^2}\left([N_\theta]^T[N_{v,\xi\xi}] + [N_{v,\xi\xi}]^T[N_\theta]\right) \\ & + \frac{A_{16}^{fg,y}}{L_e}\left([N_\theta]^T[N_{\psi,\xi}] + [N_{\psi,\xi}]^T[N_\theta]\right) + \frac{A_{16}^{gg,y}}{L_e}\left([N_\theta]^T[N_{\theta,\xi}] + [N_{\theta,\xi}]^T[N_\theta]\right) \\ & - \frac{B_{11}^{f}}{L_e^3}\left([N_{\psi,\xi}]^T[N_{w,\xi\xi}] + [N_{w,\xi\xi}]^T[N_{\psi,\xi}]\right) \\ & - \frac{B_{11}^{g}}{L_e^3}\left([N_{\theta,\xi}]^T[N_{w,\xi\xi}] + [N_{w,\xi\xi}]^T[N_{\theta,\xi}]\right) \\ & - \frac{A_{11}^{yg}}{L_e^3}\left([N_{\theta,\xi}]^T[N_{v,\xi\xi}] + [N_{v,\xi\xi}]^T[N_{\theta,\xi}]\right) \\ & + \frac{A_{11}^{fg}}{L_e^2}\left([N_{\theta,\xi}]^T[N_{\psi,\xi}] + [N_{\psi,\xi}]^T[N_{\theta,\xi}]\right) + A_{55}^{f,z^2}[N_\psi]^T[N_\psi] \Bigg] L_e d\xi \end{aligned} \quad (21)$$

Conversely, when equation 17 is substituted into equation 15, the kinetic energy of the typical element can be expressed in terms of the nodal velocity vector as:

$$T_e = \frac{1}{2}\{\dot{\delta}\}^T[M_e]\{\dot{\delta}\} \quad (22)$$

Here, $[M_e]$ denotes the element mass matrix, which can be derived as follows:

$$
\begin{aligned}
[M_e] = \int_0^1 \Bigg[& I_1([N_u]^T[N_u] + [N_v]^T[N_v] + [N_w]^T[N_w]) + \frac{I_3}{L_e^2}[N_{w,\xi}]^T[N_{w,\xi}] \\
& + \frac{I_1}{L_e^2}\frac{b^2}{12}[N_{v,\xi}]^T[N_{v,\xi}] + I_1^{f^2}[N_\psi]^T[N_\psi] + I_1^{g^2}[N_\theta]^T[N_\theta] \\
& - \frac{I_2}{L_e}\left([N_u]^T[N_{w,\xi}] + [N_{w,\xi}]^T[N_u]\right) + I_1^f\left([N_u]^T[N_\psi] + [N_\psi]^T[N_u]\right) \\
& + I_1^g([N_u]^T[N_\theta] + [N_\theta]^T[N_u]) - \frac{I_2^f}{L_e}\left([N_\psi]^T[N_{w,\xi}] + [N_{w,\xi}]^T[N_\psi]\right) \\
& - \frac{I_2^g}{L_e}\left([N_\theta]^T[N_{w,\xi}] + [N_{w,\xi}]^T[N_\theta]\right) - \frac{I_1^{yg}}{L_e}\left([N_\theta]^T[N_{v,\xi}] + [N_{v,\xi}]^T[N_\theta]\right) \\
& + I_1^{fg}\left([N_\theta]^T[N_\psi] + [N_\psi]^T[N_\theta]\right)\Bigg] L_e d\xi
\end{aligned}
\tag{23}
$$

The element mass and stiffness matrices are combined to form the total matrices $[M]$ and $[K]$, respectively. To enforce the elastic boundary conditions, the relevant elastic coefficients are inserted into the corresponding main diagonal components of the total stiffness matrices (Jafari-Talookolaei et al., 2017).

Subsequently, the discrete form of the governing equations of motion for the entire system during free vibrations is derived as:

$$[M]\{\ddot{\Delta}\} + [K]\{\Delta\} = \{0\} \tag{24}$$

Here, $\{\Delta\}$ encompasses the nodal degrees of freedom of the entire model. Assuming a general solution of $\{\Delta\} = \{\Delta_0\}e^{i\omega t}$ for equation 24, and defining $\lambda = \omega^2$, we arrive at:

$$([K] - \lambda[M])\{\Delta_0\} = \{0\} \tag{25}$$

Here, ω represents the natural frequency, and $\{\Delta_0\}$ corresponds to the mode shapes of the system. Solving equation 25 with nontrivial solutions involves solving the equation $\det([K] - \lambda[M]) = 0$, which provides the natural frequencies (eigenvalues or resonance frequencies) and the corresponding normal modes (eigenvectors) associated with the free vibration of the laminated composite beam.

4. Result and discussion

We compare the natural frequencies derived from our current model for laminated composite beams with those obtained from the commercial software ANSYS to showcase the precision of our formulations.

Unless otherwise specified, and throughout all subsequent sections, we assume a beam width of unity (i.e., $b = 1$), and all layers in the laminated beam have equal thickness. The numerical results are provided for AS4/3501 Graphite-Epoxy LCB, characterized by the following mechanical properties (Krishnaswamy et al., 1992):

$$
\begin{aligned}
& E_{11} = 144.8\ GPa, \quad E_{22} = 9.65\ GPa, \quad G_{12} = G_{13} = 4.14\ GPa \\
& G_{23} = 3.45\ GPa, \quad \nu_{12} = 0.33, \quad \rho = 1389.23\ kg/m^3
\end{aligned}
\tag{26}
$$

The calculated natural frequencies in these examples are presented in a dimensionless form as $\Omega = \omega L^2\sqrt{\rho/(E_{11}h^2)}$.

4.1. Convergence study

In order to examine the convergence of results obtained using the present finite element method, a laminated composite beam with layups [30/60/30/60] and clamped-free boundary conditions has been considered. The convergence test for the first six dimensionless frequencies of the beam is depicted in Figure 3. As observed, a very high convergence rate is evident in the finite element results.

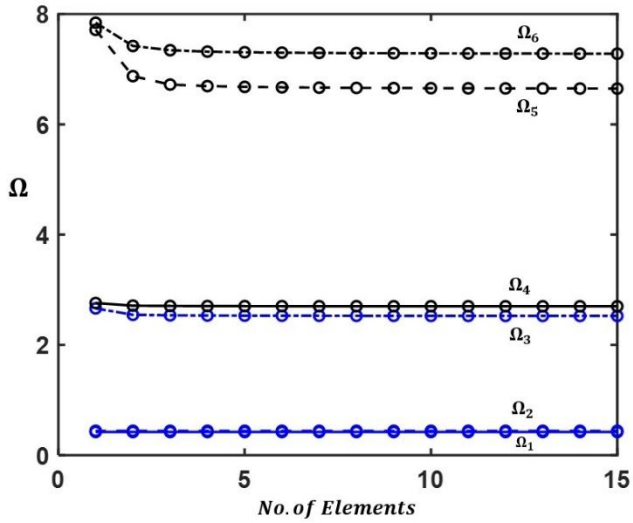

Figure 3. Convergence test for the laminated composite beam with clamped-free boundary conditions (L/h=15, [30/60/30/60], Type 5)

4.2. Laminated composite beam with different layups

To validate the accuracy of the model presented in this article, numerical results for beams with various layer orientations in this section have been compared with the results of the 3D model in the finite element software ANSYS. First three dimensionless natural frequencies for in-plane and out-of-plane bending vibrations of the beams with the cross-ply layups [0/90/0/90], [0/90/90/0], and angle-ply layups [$\theta/-\theta/\theta/-\theta$] are listed in Tables 1 to 3, respectively.

By comparing the current results with those obtained from the ANSYS software, it can be observed that the accuracy of the present mathematical model and formulations is highly suitable. This can serve as a solid foundation for future research investigations.

In Figure 4, as an illustrative example, the first six mode shapes of the laminated composite beam with [0/90/0/90] layups and type 5 are depicted.

Table 1

The first three natural frequencies for the in-plane and out-of-plane bending vibrations of the laminated beam with clamped-clamped boundary conditions (L/h=15, [0/90/0/90])

	In-plane Bending			**Out-of-plane Bending**		
Mode No.	$\boldsymbol{\Omega_1}$	$\boldsymbol{\Omega_2}$	$\boldsymbol{\Omega_3}$	$\boldsymbol{\Omega_1}$	$\boldsymbol{\Omega_2}$	$\boldsymbol{\Omega_3}$
ANSYS	3.6013	8.4503	14.2861	3.9192	9.2461	15.7126
Type 1	3.6988	8.8219	15.0952	3.9858	9.5013	16.2627
Type 2	3.6988	8.8219	15.0952	3.9858	9.5013	16.2627

	In-plane Bending			Out-of-plane Bending		
Mode No.	$\boldsymbol{\Omega_1}$	$\boldsymbol{\Omega_2}$	$\boldsymbol{\Omega_3}$	$\boldsymbol{\Omega_1}$	$\boldsymbol{\Omega_2}$	$\boldsymbol{\Omega_3}$
Type 3	3.6989	8.8263	15.1114	3.9890	9.5184	16.3078
Type 4	3.6988	8.8218	15.0943	3.9856	9.5001	16.2593
Type 5	3.7003	8.8357	15.1388	3.9941	9.5427	16.3690

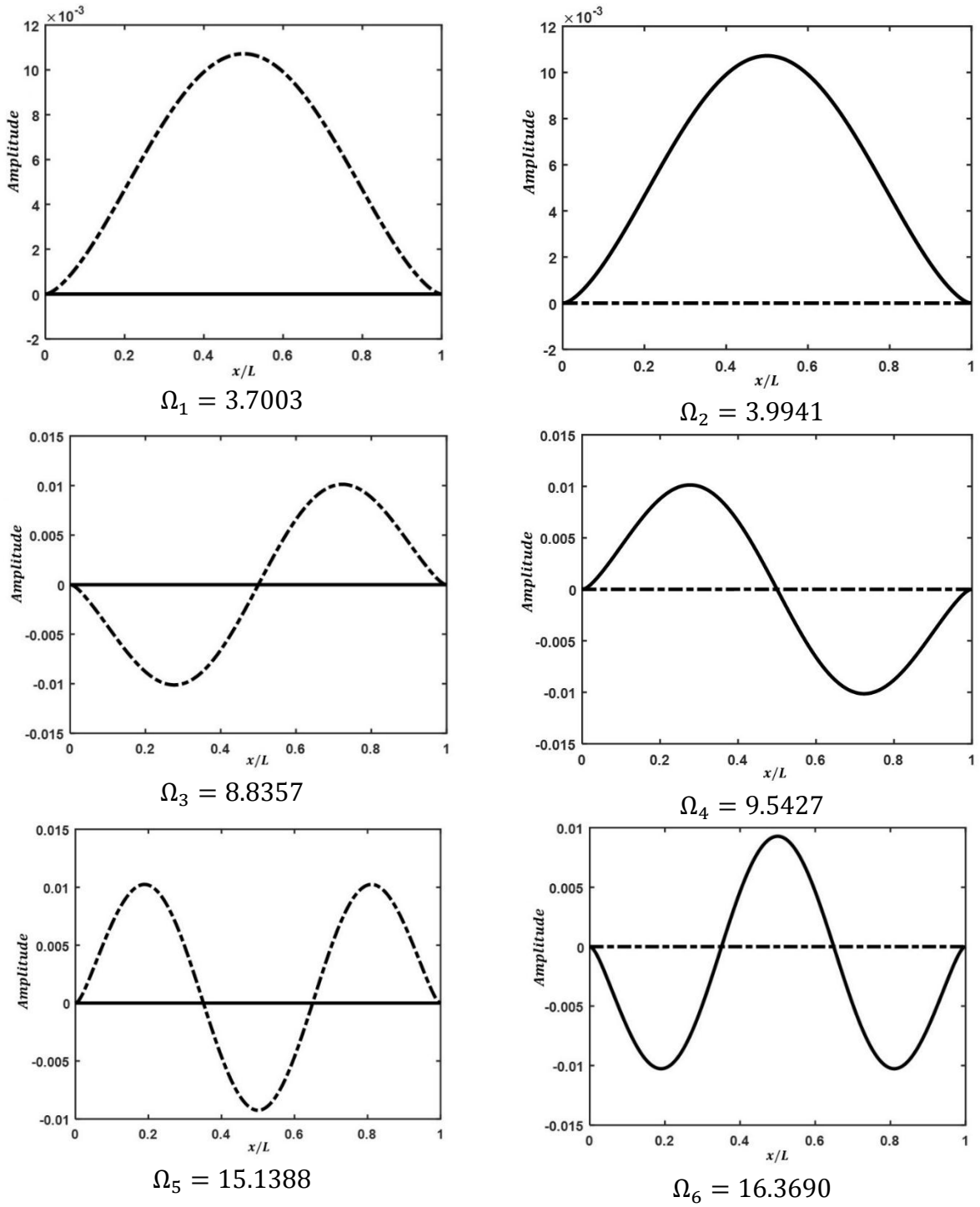

Figure 4. First six mode shapes of laminated composite beam (L/h=15, [0/90/0/90], Type 5) (Solid: v_0, Dashed-dot: w_0)

Table 2

The first three natural frequencies for the in-plane and out-of-plane bending vibrations of the laminated beam with clamped-clamped boundary conditions (L/h=15, [0/90/90/0])

	In-plane Bending			**Out-of-plane Bending**		
Mode No.	$\boldsymbol{\Omega_1}$	$\boldsymbol{\Omega_2}$	$\boldsymbol{\Omega_3}$	$\boldsymbol{\Omega_1}$	$\boldsymbol{\Omega_2}$	$\boldsymbol{\Omega_3}$
ANSYS	4.5892	10.3167	17.0576	3.9000	9.1709	15.5481
Type 1	4.6262	10.4689	17.3870	3.9858	9.5013	16.2627
Type 2	4.6262	10.4689	17.3870	3.9858	9.5013	16.2627
Type 3	4.6339	10.5004	17.4575	3.9890	9.5184	16.3078
Type 4	4.6257	10.4666	17.3817	3.9856	9.5001	16.2593
Type 5	4.6451	10.5434	17.5509	3.9941	9.5427	16.3690

Table 3

The first three natural frequencies for the in-plane and out-of-plane bending vibrations of the laminated beam with clamped-clamped boundary conditions (L/h=15, [$\theta/-\theta/\theta/-\theta$])

	In-plane Bending			**Out-of-plane Bending**		
Mode No.	$\boldsymbol{\Omega_1}$	$\boldsymbol{\Omega_2}$	$\boldsymbol{\Omega_3}$	$\boldsymbol{\Omega_1}$	$\boldsymbol{\Omega_2}$	$\boldsymbol{\Omega_3}$
$\theta = 0$						
ANSYS	4.8639	10.9133	18.0264	4.8745	10.9529	18.1150
Type 1	4.8980	11.0761	18.4029	4.8981	11.0766	18.4018
Type 2	4.8980	11.0761	18.4018	4.8981	11.0766	18.4029
Type 3	4.9059	11.1125	18.4888	4.9060	11.1129	18.4898
Type 4	4.8974	11.0733	18.3950	4.8975	11.0738	18.3961
Type 5	4.9173	11.1605	18.6011	4.9174	11.1609	18.6002
$\theta = 15$						
ANSYS	4.0427	9.4002	15.8745	4.4666	11.4592	20.4220
Type 1	4.4182	10.2247	17.2438	5.2424	13.0458	22.6600
Type 2	4.4182	10.2247	17.2438	5.2424	13.0458	22.6600
Type 3	4.4266	10.2521	17.3040	5.2446	13.0598	22.7073
Type 4	4.4176	10.2227	17.2394	5.2423	13.0449	22.6567
Type 5	4.4380	10.2896	17.3848	5.2483	13.0809	22.7750
$\theta = 30$						
ANSYS	2.7923	6.9390	12.2369	2.8753	7.8071	14.9745
Type 1	3.1052	7.7232	13.6323	3.5088	9.3159	17.3891
Type 2	3.1052	7.7232	13.6323	3.5088	9.3159	17.3891

	In-plane Bending			**Out-of-plane Bending**		
Mode No.	$\boldsymbol{\Omega_1}$	$\boldsymbol{\Omega_2}$	$\boldsymbol{\Omega_3}$	$\boldsymbol{\Omega_1}$	$\boldsymbol{\Omega_2}$	$\boldsymbol{\Omega_3}$
Type 3	3.1098	7.7358	13.6582	3.5091	9.3180	17.3977
Type 4	3.1048	7.7222	13.6305	3.5088	9.3158	17.3886
Type 5	3.1156	7.7533	13.6952	3.5097	9.3217	17.4118
$\theta = 45$						
ANSYS	1.9338	5.0480	9.2975	1.9539	5.3294	10.2971
Type 1	1.9577	5.1399	9.5173	2.0463	5.5183	10.5151
Type 2	1.9577	5.1399	9.5173	2.0463	5.5183	10.5151
Type 3	1.9589	5.1435	9.5254	2.0464	5.5188	10.5167
Type 4	1.9577	5.1396	9.5167	2.0463	5.5183	10.5151
Type 5	1.9604	5.1486	9.5373	2.0465	5.5197	10.5198
$\theta = 60$						
ANSYS	1.6440	4.3590	8.1532	1.6710	4.5408	8.7325
Type 1	1.6296	4.3285	8.1123	1.6534	4.4539	8.4784
Type 2	1.6296	4.3285	8.1123	1.6534	4.4539	8.4784
Type 3	1.6298	4.3294	8.1152	1.6534	4.4543	8.4797
Type 4	1.6296	4.3284	8.1121	1.6534	4.4539	8.4783
Type 5	1.6301	4.3312	8.1204	1.6536	4.4551	8.4823
$\theta = 75$						
ANSYS	1.6078	4.2680	7.9922	1.6284	4.3859	8.3469
Type 1	1.6063	4.2662	7.9951	1.6184	4.3318	8.1868
Type 2	1.6063	4.2662	7.9951	1.6184	4.3318	8.1868
Type 3	1.6064	4.2671	7.9979	1.6185	4.3324	8.1887
Type 4	1.6063	4.2662	7.9950	1.6184	4.3318	8.1867
Type 5	1.6067	4.2687	8.0028	1.6187	4.3335	8.1924
$\theta = 90$						
ANSYS	1.6154	4.2859	8.0205	1.6236	4.3305	8.1525
Type 1	1.6161	4.2893	8.0323	1.6237	4.3306	8.1524
Type 2	1.6161	4.2893	8.0323	1.6237	4.3306	8.1524
Type 3	1.6162	4.2901	8.0351	1.6238	4.3313	8.1547
Type 4	1.6161	4.2892	8.0321	1.6237	4.3306	8.1523
Type 5	1.6165	4.2918	8.0402	1.6241	4.3327	8.1590

4.3. Influence of width to thickness ratio and boundary conditions

In this section, the effect of the beam's width-to-thickness ratio (b/h) on the dimensionless frequencies of in-plane and out-of-plane bending vibrations of the laminated composite beam with different boundary conditions has been investigated. The beam is composed of layers with [30/60/30/60] stacking sequence, and the length-to-thickness ratio is set to $L/h = 15$. Without the lack of generality, the displacement field of type 3 has been considered. It should be mentioned that to extract the results for different values of b/h, the thickness (h) has been kept constant while the width (b) is varied.

As observed, an increase in the b/h ratio does not significantly alter the in-plane bending frequency for all boundary conditions. However, there is a noticeable increase in the out-of-plane bending frequency. Furthermore, the results indicate that initially, the in-plane frequency is higher than the out-of-plane frequency. However, within the b/h range of 0.9 to 1 and depending on the type of boundary conditions, this order is reversed, and the out-of-plane frequency surpasses the in-plane frequency.

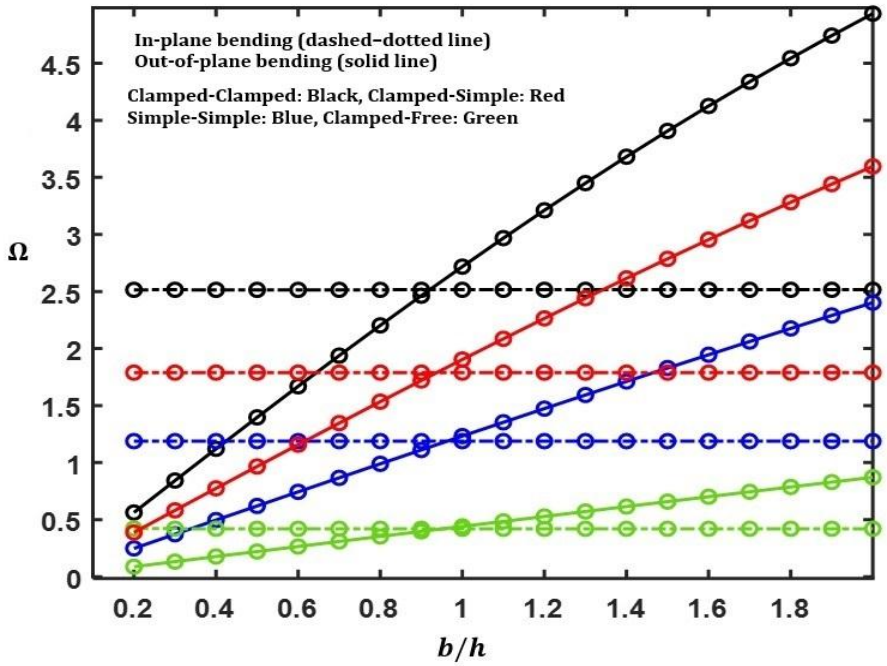

Figure 5. The influence of the beam's width to thickness ratio (b/h) on the dimensionless fundamental frequencies of the laminated beam (*L/h*=15, [30/60/30/60], Type 3)

4.4. Effects of slenderness ratio and material anisotropy

In this section, the effects of the slenderness ratio (L/h) and the anisotropy ratio (E_{11}/E_{22}) on the in-plane and out-of-plane bending frequencies have been investigated, and the corresponding results are shown in Figures 6 and 7, respectively. In both cases, a beam with clamped-clamped boundary conditions, displacement field type 5, and the stacking sequence [30/60/30/60] has been considered.

It is worth noting that, in obtaining the results in Figure 6, the thickness (h) was kept constant while the length (L) was varied. As observed, with an increase in the slenderness ratio, the dimensionless frequencies increase and then tend towards a constant value, which corresponds to the frequency obtained based on the classical theory.

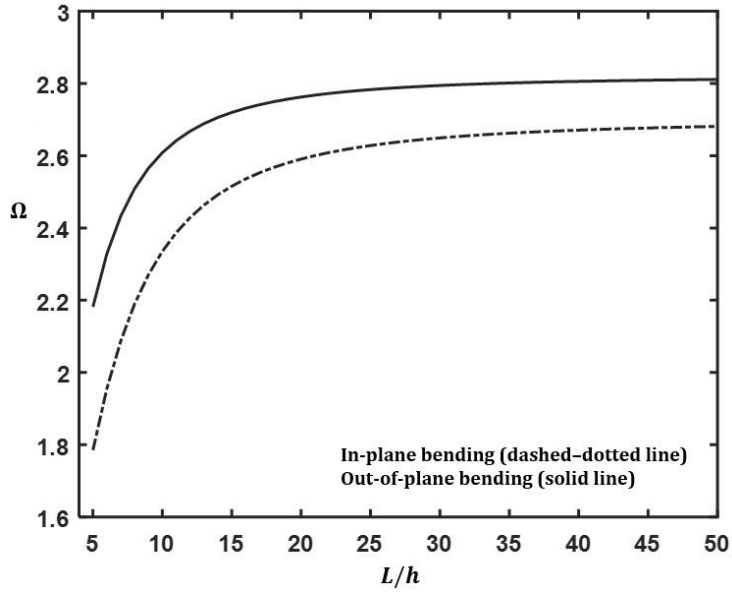

Figure 6. The influence of slenderness ratio (*L/h*) on the dimensionless fundamental frequencies of the laminated beam (Clamped-clamped boundary conditions, [30/60/30/60], Type 5)

It should be noted that, in extracting the dimensionless frequencies in Figure 7, the value of E_{22} was held constant and calculated based on equation 26, while the value of E_{11} was varied. Additionally, in obtaining the dimensionless frequencies (Ω) in this figure, E_{11} has been replaced using equation 26. It has been observed that an increase in the anisotropy ratio leads to higher in-plane and out-of-plane bending frequencies. The rate of this increase is initially steep but gradually diminishes. Additionally, as the aspect ratio increases, the difference between these frequencies also becomes more pronounced.

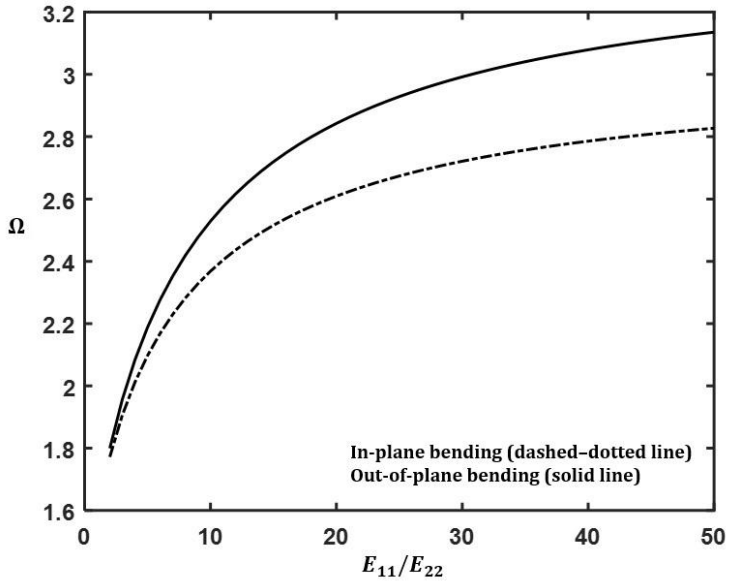

Figure 7. Influence of material anisotropy (E_{11}/E_{22}) on the dimensionless fundamental frequencies of the laminated beam (*L/h*=15, clamped-clamped boundary conditions, [30/60/30/60], Type 5)

5. Conclusions

This paper presents the in-plane and out-of-plane free vibration analysis of laminated composite beams using novel higher-order displacement fields, accounting for Poisson's ratio, shear deformation, and rotary inertia. A new finite element was introduced to determine the vibration characteristics, and the results were compared with those from 3D ANSYS software.

The main findings are as follows:

- The results show close agreement with those obtained from ANSYS, validating the proposed method.

- For a *b/h* ratio ranging from 0.9 to 1, the in-plane bending frequency initially exceeds the out-of-plane frequency. However, as the ratio approaches 1, the out-of-plane frequency surpasses the in-plane frequency, depending on the boundary conditions.

- An increase in the slenderness ratio leads to an increase in dimensionless frequencies, which then level off to a constant value.

- With a higher anisotropy ratio, both in-plane and out-of-plane bending frequencies increase rapidly at first, then at a slower rate. The difference between these frequencies also grows with an increasing aspect ratio.

References

Alazwari, M. A., Mohamed, S. A., & Eltaher, M. A. (2022). Vibration analysis of laminated composite higher order beams under varying axial loads. *Ocean Engineering, 252,* Article 111203.

Ambartsumyan, S. (1958). On theory of bending plates. *Izvestiya Akademii Nauk SSSR, Seriya Khimicheskaya, 5*(5), 69-77.

Aydogdu, M. (2006). Free vibration analysis of angle-ply laminated beams with general boundary conditions. *Journal of Reinforced Plastics and Composites, 25*(15), 1571-1583.

Belabed, Z., Tounsi, A., Al-Osta, M. A., Tounsi, A., & Le, M. H. (2024). On the elastic stability and free vibration responses of functionally graded porous beams resting on Winkler Pasternak foundations via finite element computation. *Geomechanics and Engineering, 36*(2), 183-204.

Belabed, Z., Tounsi, A., Bousahla, A. A., Tounsi, A., Bourada, M., & Al-Osta M.A. (2024). Free vibration analysis of Bi-Directional Functionally Graded Beams using a simple and efficient finite element model. *Structural Engineering and Mechanics, 90*(3), 233-252.

Boukhalfa, A., Hadjoui, A., & Cherif, S. M. H. (2008). Free vibration analysis of a rotating composite shaft using the p-version of the finite element method. *International Journal of Rotating Machinery,* Article 752062.

Bui, B. X., Nguyen, K. T., Nguyen, D. N., & Vo, P. T. (2022). A general higher-order shear deformation theory for buckling and free vibration analysis of laminated thin-walled composite I-beams. *Composite Structures, 295,* Article 115775.

Bui, C. M., Tounsi, A., Do, T. V., Nguyen, V. T. H., & Phung, M. V. (2024). Finite element modelling for the static bending response of rotating FG-GPLRC beams with geometrical imperfections in thermal mediums. *Computers and Concrete, 33*(1), 91-102.

Chandiramani, N. K., Librescu, L., & Shete, C. D. (2002). On the free-vibration of rotating composite beams using a higher-order shear formulation. *Aerospace Science and Technology, 6*(8), 545-561.

Chandrashekhara, K., Krishnamurthy, K., & Roy, S. (1990). Free vibration of composite beams including rotary inertia and shear deformation. *Composite Structures, 14*(4), 269-279.

Dao, T. M., Do, T. V., Nguyen, V. T. H., Tounsi, A., Phung, M. V., & Dao, M. N. (2023). Buckling and forced oscillation of organic nanoplates taking the structural drag coefficient into account. *Computers and Concrete, 32*(6), 553-565.

Groh, R. M. J., & Weaver, P. M. (2015). Static inconsistencies in certain axiomatic higher-order shear deformation theories for beams, plates and shells. *Composite Structures, 120*, 231-245.

Hijmissen, J. W., & Van Horssen, W. T. (2008). On transverse vibrations of a vertical Timoshenko beam. *Journal of Sound and Vibration, 314*(1/2), 161-179.

Jafari-Talookolaei, R.-A., Abedi, M., & Attar, M. (2017). In-plane and out-of-plane vibration modes of laminated composite beams with arbitrary lay-ups. *Aerospace Science and Technology, 66*, 366-379.

Jafari-Talookolaei, R.-A., Abedi, M., Kargarnovin, M. H., & Ahmadian, M. T. (2012). An analytical approach for the free vibration analysis of generally laminated composite beams with shear effect and rotary inertia. *International Journal of Mechanical Sciences, 65*(1), 97-104.

Jafari-Talookolaei, R.-A., Attar, M., Valvo, P. S., Lotfinejad-Jalali, F., Shirsavar, S. F. G., & Saadatmorad M. (2022). Flapwise and chordwise free vibration analysis of a rotating laminated composite beam. *Composite Structures, 292*, Article 115694.

Kant, T., & Gupta, A. (1988). A finite element model for a higher-order shear-deformable beam theory. *Journal of Sound and Vibration, 125*(2), 193-202.

Kant, T., Marur, S. R., & Rao, G. S. (1998). Analytical solution to the dynamic analysis of laminated beams using higher order refined theory. *Composite Structures, 40*(1), 1-9.

Karama, M., Afaq, K. S., & Mistou, S. (2003). Mechanical behaviour of laminated composite beam by the new multi-layered laminated composite structures model with transverse shear stress continuity. *International Journal of Solids and Structures, 40*(6), 1525-1546.

Kim, S., Kim, K., Ri, M., Paek, Y., & Kim, C. (2021). A semi-analytical method for forced vibration analysis of cracked laminated composite beam with general boundary condition. *Journal of Ocean Engineering and Science, 6*(1), 40-53.

Krishnaswamy, S., Chandrashekhara, K., & Wu, W. Z. B. (1992). Analytical solutions to vibration of generally layered composite beams. *Journal of Sound and Vibration, 159*(l), 85-99.

Lakhdar, Z., Chorfi, S. M., Belalia, S. A., Khedher, K. M., Alluqmani, A. E., Tounsi, A., & Yaylacı, M. (2024). Free vibration and bending analysis of porous bi-directional FGM sandwich shell using a TSDT p-version finite element method. *Acta Mechanica, 235*, 3657-3686.

Matsunaga, H. (2001). Vibration and buckling of multilayered composite beams according to higher order deformation theories. *Journal of Sound and Vibration, 246*(1), 47-62.

Matsunaga, H. (2002). Interlaminar stress analysis of laminated composite beams according to global higher-order deformation theories. *Composite Structures, 55*(1), 105-114.

Meftah, S. A., Aldosari, S. M., Tounsi, A., Le, C. T., Khedher, K. M., & Alluqmani, A. E. (2024). Simplified homogenization technique for nonlinear finite element analysis of in-plane loaded masonry walls. *Engineering Structures, 306*, Article 117822.

Mesbah, A., Belabed Z., Amara, K., Tounsi, A., Bousahla, A. A., & Bourada, F. (2023). Formulation and evaluation a finite element model for free vibration and buckling behaviours of Functionally Graded Porous (FGP) beams. *Structural Engineering and Mechanics, 86*(3), 291-309.

Nguyen, K. T., Nguyen, D. B., Vo, P. T., & Thai, T. H. (2020). A novel unified model for laminated composite beams. *Composite Structures, 238*, Article 111943.

Pavan, G. S., Muppidi, H., & Dixit, J. (2022). Static, free vibrational and buckling analysis of laminated composite beams using isogeometric collocation method. *European Journal of Mechanics - A/Solids, 96*, Article 104758.

Pham, V. V., Nguyen, C. V., & Tounsi, A. (2022). Static bending and buckling analysis of bi-directional functionally graded porous plates using an improved first-order shear deformation theory and FEM. *European Journal of Mechanics - A/Solids, 96*, Article 104743.

Reddy, J. N. (1986). *A refined shear deformation theory for the analysis of laminated plates* (Contractor Report 3955). Retrieved March 28, 2024, from https://ntrs.nasa.gov/api/citations/19860007138/ downloads/19860007138.pdf

Reddy, J. N. (2004). *Mechanics of laminated composite plates and shells: Theory and analysis.* Boca Raton, FL: CRC Press.

Ren, S., Cheng, C., Meng, Z., Yu, B., & Zhao, G. (2021). A new general third-order zigzag model for asymmetric and symmetric laminated composite beams. *Composite Structures, 260*, Article 113523.

Seraj, S., & Ganesan, R. (2018). Dynamic instability of rotating doubly-tapered laminated composite beams under periodic rotational speeds. *Composite Structures, 200*, 711-728.

So, S.-R., Yun, H., Ri, Y., Ryongsik, O., & Yun, Y. (2021). Haar wavelet discretization method for free vibration study of laminated composite beam under generalized boundary conditions. *Journal of Ocean Engineering and Science, 6*(1), 1-11.

Soldatos, K. (1992). A transverse shear deformation theory for homogeneous monoclinic plates. *Acta Mechanica, 94*, 195-220.

Subramanian, P. (2006). Dynamic analysis of laminated composite beams using higher order theories and finite elements. *Composite Structures, 73*(3), 342-353.

Touratier, M. (1991). An efficient standard plate theory. *International Journal of Engineering Science, 29*(8), 901-916.

Zhen, W., & Wanji, C. (2008). An assessment of several displacement-based theories for the vibration and stability analysis of laminated composite and sandwich beams. *Composite Structures, 84*(4), 337-349.